Effect of substrates on the molecular orientation of silicon phthalocyanine dichloride thin films

2007 J. Phys.: Condens. Matter 19 196205

(http://iopscience.iop.org/0953-8984/19/19/196205)

IOP PUBLISHING JOURNAL OF PHYSICS: CONDENSED MATTER

J. Phys.: Condens. Matter **19** (2007) 196205 (11pp) doi:10.1088/0953-8984/19/19/196205

Effect of substrates on the molecular orientation of silicon phthalocyanine dichloride thin films

Juzhi Deng[1,2], **Yuji Baba**[1,3], **Tetsuhiro Sekiguchi**[1], **Norie Hirao**[1] and **Mitsunori Honda**[1]

[1] Japan Atomic Energy Agency, Tokai-mura, Naka-gun, Ibaraki-ken 319-1195, Japan
[2] Key Laboratory of Nuclear Resources and Environment (East China Institute of Technology), Ministry of Education, Nanchang 330013, People's Republic of China

E-mail: baba.yuji@jaea.go.jp

Received 12 March 2007
Published 18 April 2007
Online at stacks.iop.org/JPhysCM/19/196205

Abstract

Molecular orientations of silicon phthalocyanine dichloride ($SiPcCl_2$) thin films deposited on three different substrates have been measured by near-edge x-ray absorption fine structure (NEXAFS) spectroscopy using linearly polarized synchrotron radiation. The substrates investigated were highly oriented pyrolitic graphite (HOPG), polycrystalline gold and indium tin oxide (ITO). For thin films of about five monolayers, the polarization dependences of the Si K-edge NEXAFS spectra showed that the molecular planes of $SiPcCl_2$ on three substrates were nearly parallel to the surface. Quantitative analyses of the polarization dependences revealed that the tilted angle on HOPG was only 2°, which is interpreted by the perfect flatness of the HOPG surface. On the other hand, the tilted angle on ITO was 26°. Atomic force microscopy (AFM) observation of the ITO surface showed that the periodicity of the horizontal roughness is of the order of a few nanometres, which is larger than the molecular size of $SiPcCl_2$. It is concluded that the morphology of the top surface layer of the substrate affects the molecular orientation of $SiPcCl_2$ molecules not only for mono-layered adsorbates but also for multi-layered thin films.

1. Introduction

Organic semiconductor thin films have been receiving an increasing amount of attention in recent years. This interest can be attributed to their promising potential for optical and photoelectronic devices [1, 2]. Among the organic molecules, metal phthalocyanines (MPc) have been widely employed in the preparation of heterostructures as substrate metals [3], semiconductors [4], and layered materials [5]. Furthermore, MPc molecules show a high

[3] Author to whom any correspondence should be addressed.

0953-8984/07/196205+11$30.00

thermal stability and a low vapour pressure, thus representing a suitable choice for growing ultrathin films in UHV conditions.

It has already been predicted that silicon phthalocyanine (SiPc) derivatives, together with some metal phthalocyanines, form electric conducting molecules if the molecules are stacked face-to-face and provide a coaxially contiguous pathway for carrier delocalization [6–9]. It has been reported that the molecular orientation of some of the MPcs depends on the nature of the substrates [10–13]. So it is important to elucidate the ordering and orientation of SiPc molecules on different substrate in order to determine their device properties [14].

In the present work, we investigate the molecular ordering and orientation of thin films of silicon phthalocyanine dichloride ($SiPcCl_2$) deposited on different substrates. Three substrates were used in this study: highly oriented pyrolytic graphite (HOPG), polycrystalline gold, and indium tin oxide (ITO). An HOPG substrate was chosen because it has chemically inert and ideally flat surface. Gold and ITO substrates were chosen as typical examples of an electric wire and a substrate, respectively, with high electric conductivity. These materials are already used in practical device processing. The molecular orientations were investigated by near-edge x-ray absorption fine structure (NEXAFS) spectroscopy using linearly polarized x-rays from synchrotron light source. NEXAFS spectroscopy is one of the powerful tools to elucidate the molecular orientations of the adsorbed molecules, because there are strict dipole-selection rules for the core-to-valence resonant excitations that make the absorption intensity strongly anisotropic for oriented molecules [15]. Using polarized x-rays from synchrotron light source, we can assign the orientation of the molecules on solid surfaces simply by changing the angle of the incident x-rays [16, 17]. The observed differences in the molecular orientations between three substrates are discussed on the basis of the surface morphology of the substrates.

2. Experiments

NEXAFS and x-ray photoelectron spectroscopy (XPS) were conducted at the soft x-ray beamline 27 A at the Photon Factory of the High-Energy Accelerator Research Organization (KEK-PF), Tsukuba, Japan. The beam line was equipped with an InSb(111) double-crystal monochromator. The energy resolution from the monochromator was 0.85 eV at 1.84 keV (Si K-edge). The x-rays from the synchrotron light source were generated in the bending magnet, so they were linearly polarized in the horizontal direction.

The end station had two vacuum chambers: a main chamber for NEXAFS and XPS measurements, and a preparation chamber for synthesis of the samples. The base pressure of both chambers was on the order of 10^{-8} Pa. The main chamber consisted of a hemispherical electron energy analyser (VSW Co., Class-100) for XPS measurements, a five-axis manipulator and a YAG-laser annealing system. In the preparation chamber, a Knudsen cell (K-cell) evaporator, a quartz crystal thickness monitor and a sample transfer system were installed [18].

Powder samples of $SiPcCl_2$ were purchased from Sigma-Aldrich Co. The chemical structure of $SiPcCl_2$ is shown in figure 1. The molecular size of the plane is 1.2 nm. The HOPG samples were purchased from Tomoe Co. and the sample was cleaved just before introducing it into the vacuum chamber. The ITO sample was obtained form Kuramoto Co. The polycrystalline ITO was deposited on a glass plate at a thickness of 240 nm. ITO and polycrystalline gold substrates were cleaned with acetone by ultrasonication. The $SiPcCl_2$ films were deposited on the substrates using K-cell evaporator. All the evaporation sources were well degassed before deposition. The substrates were kept at room temperature during deposition. The rate of deposition was monitored using the quartz crystal thickness monitor. The thickness of the deposited layer was also determined from the XPS peak intensities. We prepared the three samples at the same time, which means that the thicknesses of the films on

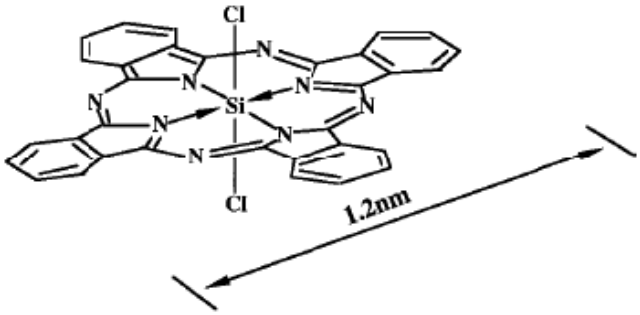

Figure 1. Molecular structure of $SiPcCl_2$.

the three substrates were the same. The pressure during the deposition of $SiPcCl_2$ film was 1×10^{-6} Pa. For comparison, powdered $SiPcCl_2$ samples attached to HOPG before and after heating with laser were also measured.

The NEXAFS spectra at the Si K-edge region were taken by plotting the sample drain current as a function of photon energy. The photon flux was always monitored by the current in the aluminium foil, located in front of the sample. This method is called the total electron yield (TEY) mode. The base pressure during the NEXAFS measurements was 1×10^{-7} Pa. For the measurements of the polarization dependences, the sample was rotated around the vertical axis. The incidence angle θ of the x-rays relative to the substrate surface was changed from the glancing angle ($\theta = 15°$) to near normal incidence ($\theta = 80°$). The photon energy was calibrated using the Si 1s $\rightarrow \sigma^*$ resonance peak for SiO_2 [19].

The surface morphologies of the substrates were observed by atomic force microscopy (AFM) using a nano-scale hybrid microscope from Keyence Co. The vertical space resolution of the AFM was 0.3 nm.

3. Results and discussion

3.1. X-ray photoelectron spectra

Before showing the NEXAFS results, we first describe how we evaluated the thickness d of the films that we prepared using the vacuum evaporation method. Figure 2 shows the XPS semi-wide scan spectra excited by 2200 eV photons for $SiPcCl_2$ molecules deposited on Au. The assignments of the peaks are indicated in the figure, which include photoelectrons from substrate gold (Au 4f, and Au 3d) and molecules $SiPcCl_2$ (N 1s and C 1s). As expected, the $I(\text{N 1s})/I(\text{Au 4f})$ ratio increases with an increase in sample thickness. For homogeneous thin films covering the gold substrate, the intensity of the N 1s photoelectron, $I(\text{N 1s})$, is expressed as

$$I(\text{N1s}) = K\sigma(\text{N1s})\lambda_{\text{SiPcCl}_2}(\text{N1s})n_{\text{SiPcCl}_2}(\text{N}) \times \left[1 - \exp\left\{\frac{-d}{\lambda_{\text{SiPcCl}_2}(\text{N1s})}\right\}\right], \tag{1}$$

where K is a constant that depends on the detection efficiency and the x-ray flux, $\sigma(\text{N 1s})$ is the photoionization cross section of N 1s for 2200 eV photons, $\lambda_{\text{SiPcCl}_2}(\text{N 1s})$ is the inelastic mean free path (IMFP) of the N 1s photoelectron in $SiPcCl_2$, and n (N) is the atomic concentration of nitrogen in the $SiPcCl_2$ sample [20]. For gold, the Au 4f photoelectrons $I(\text{Au 4f})$ is calculated as

$$I(\text{Au 4f}) = K\sigma(\text{Au 4f})\lambda_{\text{Au}}(\text{Au 4f})n_{\text{Au}}(\text{Au}) \exp\left\{\frac{-d}{\lambda_{\text{SiPcCl}_2}(\text{Au 4f})}\right\}, \tag{2}$$

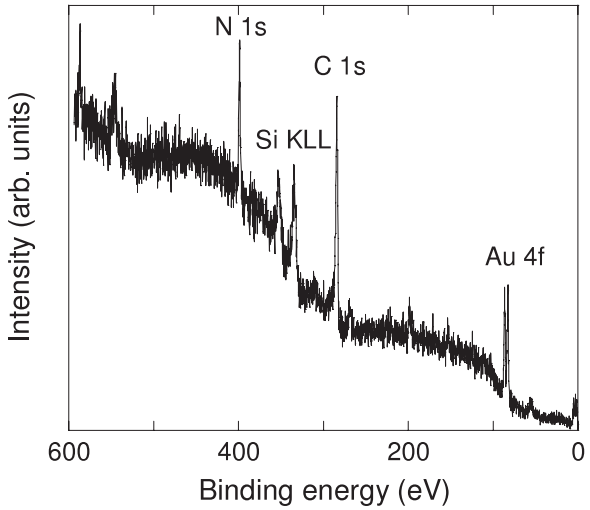

Figure 2. XPS semi-wide scan excited by 2200 eV photons for $SiPcCl_2$ thin films on Au. The thickness of the thin sample obtained from this spectrum is 2.56 nm.

where all of the parameters are the same as those in the equation (1). For σ, the reported values were used [21]. Using the TTP-2M equation [22], the values λ_{SiPcCl_2}(N1 s), λ_{Au}(Au 4f) and λ_{SiPcCl_2}(Au 4f) were estimated to be 0.47, 8.2 and 0.51 nm, respectively. For the sample shown in figure 2, the I(N1s)/I(Au 4f) ratio in the XPS spectrum is 0.272, so we obtain $d = 2.56$ nm. The error in the estimation of the film thickness was roughly 8%. Considering that the height of one monolayer is 0.54 nm [23], the film thickness of this sample is estimated to be five molecular layers.

3.2. Si K-edge NEXAFS spectra

Figure 3 shows the Si K-edge NEXAFS spectra for $SiPcCl_2$ on the HOPG surface. The spectrum (c) represents the thin $SiPcCl_2$ sample on HOPG prepared using the vacuum deposition method. For comparison, the spectrum for the powdered $SiPcCl_2$ sample mechanically attached onto the HOPG surface is shown as (a). The spectrum (b) represents the powdered $SiPcCl_2$ sample on HOPG after heating at ∼345 °C for 5 min in vacuum using a laser. The symbol 'θ', as shown in the inset of figure 3, represents the angle between the incident x-ray beam axis and the surface plane; the angle θ is also equal to the angle between the surface normal ($\vec{n}$) and the electric field vector ($\boldsymbol{E}$) of the x-rays.

For the samples heated in the vacuum (b), a new clear peak was observed at 1843.1 eV, while the shoulder at 1845.8 eV disappeared. This result indicates that the $SiPcCl_2$ molecule was decomposed by heating at ∼345 °C. However, there are no differences between powdered sample (a) and the sample prepared by vacuum deposition (c). The results show that $SiPcCl_2$ molecules are evaporated in molecular form without decomposing by heat. Thus it was elucidated that the vacuum deposition method is effective in producing thin films of $SiPcCl_2$ molecules.

In table 1, the XPS binding energies for $SiPcCl_2$ on HOPG prepared by three different conditions are shown. For the sample heated in vacuum, the Cl 1 s peak is located at ∼2823.5 eV, which is about 1 eV higher than those of the other two samples. Although the exact chemical states after heating remains unclear, the XPS results suggest that the Si–Cl bonds

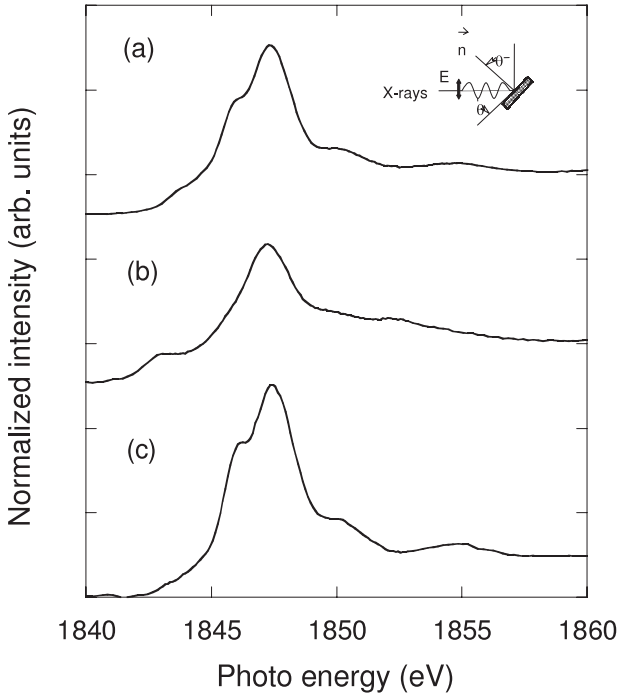

Figure 3. NEXAFS spectra at the silicon K-edge taken by total electron yield: (a) powdered $SiPcCl_2$ sample before heating; (b) powdered $SiPcCl_2$ sample on HOPG after heating at ∼345° for 5 min in vacuum with a laser; (c) thin $SiPcCl_2$ sample on HOPG prepared by vacuum deposition method. E is the electric field vector of the synchrotron beam, and θ is the incident angle defined by the angle between the sample surface and the synchrotron beam.

Table 1. XPS binding energies (eV) for $SiPcCl_2$ on HOPG prepared under three different conditions.

	Powder without heating	Powder heated at 345 °C in vacuum	Deposited in vacuum
Si 1s	1844.5	1844.5	1844.5
Cl 1s	2822.3	2823.5	2822.5
N 1s	399.1	399.2	399.1
C 1s	284.3	284.3	284.3

are changed to the other structures due to the cleavage of the Si–Cl bond. The disappearance of the 1845.8 eV shoulder in figure 3(b) coincides with the XPS results, because this shoulder originates from the resonance excitation from the Si 1s to the unoccupied σ^* orbitals located around the Si–Cl bond, as discussed later.

The silicon K-edge NEXAFS spectra for $SiPcCl_2$ films on HOPG, gold and ITO substrates are shown in the upper parts of figures 4–6, respectively. In all figures, three spectra at three different incidence angles are shown. It is noteworthy that the NEXAFS spectra for all substrates exhibit strong polarization dependences, from near-normal (80°) to grazing (15°) incidences. For all substrates, the first peaks (labelled A) exhibit the opposite angular dependence to the second peaks (labelled B). Peaks A have maximum intensities at grazing incidence, while peaks B have maximum intensities at near-normal incidence.

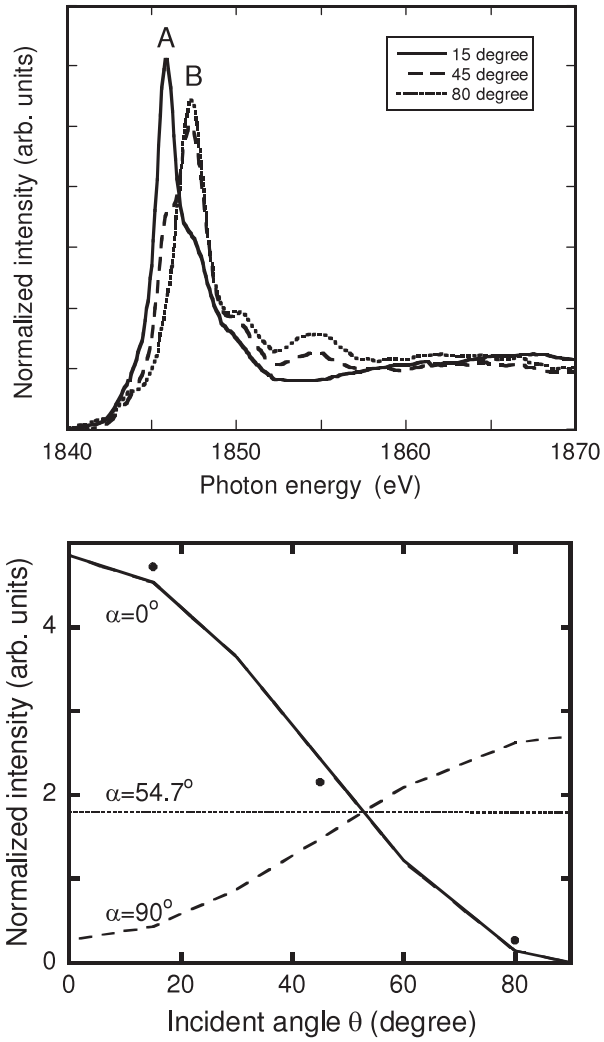

Figure 4. Upper figure: polarization dependence of NEXAFS spectra at the silicon K-shell for the $SiPcCl_2$ molecules deposited on HOPG substrate. Lower figure: intensity $I(\theta)$ of the σ^*_{Si-Cl} resonance peak in the Si K-edge NEXAFS spectra as a function of the x-ray incidence (polarization) angle θ. The substrate is HOPG. The best-fit curve is shown as a solid line. Also shown are theoretical curves calculated with three different tilted angles, i.e. 0° (chain lines), 54.7° (dotted lines) and 90° (broken lines).

In order to assign the origins of these peaks, we have conducted theoretical calculations on the unoccupied molecular orbitals in the core excited states (equivalent core approximation) [24] for $SiPcCl_2$ molecules using the self-consistent field molecular orbital (SCF-MO) method with the 3-21G basis set [25, 26]. The most stable molecular structures were obtained by optimizing the total potential energy. Based on the calculations, we assigned the peak A as the resonance excitation from the Si 1s into the unoccupied σ^* orbitals located around the Si–Cl bonds, while the peak B is due to the resonance excitation from the Si 1s into the unoccupied σ^* orbitals located around the Si–N bonds [27]. It should be noted that the direction of the Si–Cl bond is out-of-plane, while that of the Si–N bond is in the plane of the flat

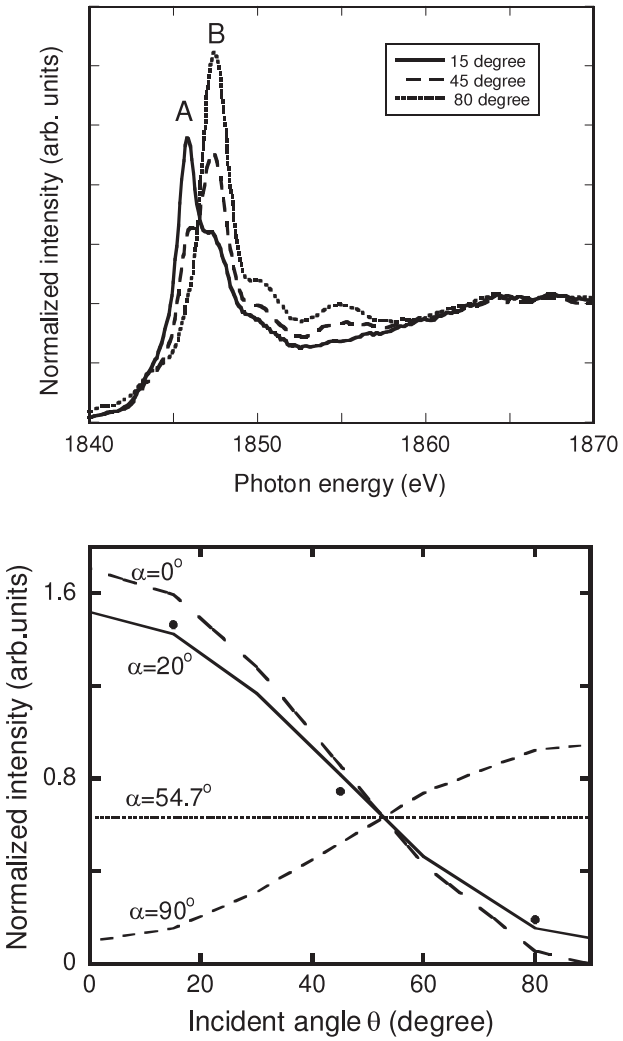

Figure 5. Upper figure: polarization dependence of NEXAFS spectra at the silicon K-shell for the $SiPcCl_2$ molecules deposited on Au substrate. Lower figure: intensity $I(\theta)$ of the σ^*_{Si-Cl} resonance peak in the Si K-edge NEXAFS spectra as a function of the x-ray incidence (polarization) angle θ. The substrate is gold. The best-fit curve is shown as a solid line. Also shown are theoretical curves calculated with three different tilted angles, i.e. 0° (chain lines), 54.7° (dotted lines) and 90° (broken lines).

$SiPcCl_2$ molecule (see figure 1). So we can determine the molecular orientation by analysing the polarization dependences of the two peak intensities, as follows.

The intensity of peak A decreases with the increase in the incidence angles of the synchrotron beam. In contrast, the intensity of peak B increases with the increase in the incidence angles. The peak intensity I of the NEXAFS spectra using the synchrotron beam of electric field E is expressed as,

$$I \propto |E \cdot O|^2 \propto \cos^2 \delta \tag{3}$$

where O is the direction of the final state orbital and δ is the angle between E and O [28]. Thus, the polarization dependences in figures 4–6 indicate that the final state orbitals represented by

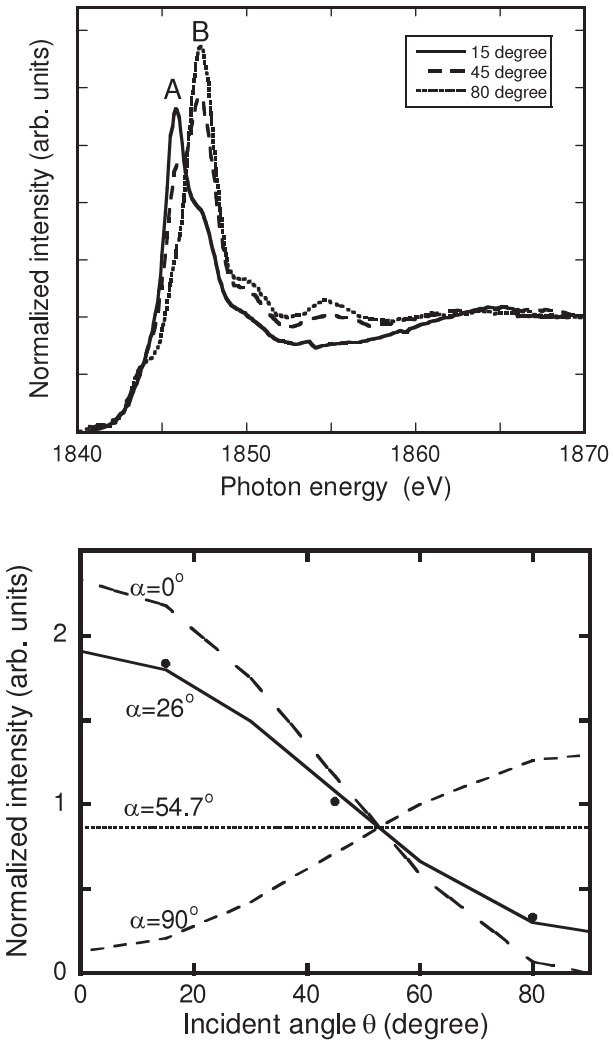

Figure 6. Upper figure: polarization dependence of NEXAFS spectra at the silicon K-shell for the $SiPcCl_2$ molecules deposited on ITO substrate. Lower figure: intensity $I(\theta)$ of the σ^*_{Si-Cl} resonance peak in the Si K-edge NEXAFS spectra as a function of the x-ray incidence (polarization) angle θ. The substrate is ITO. The best-fit curve is shown as a solid line. Also shown are theoretical curves calculated with three different tilted angles, i.e. 0° (chain lines), 54.7° (dotted lines) and 90° (broken lines).

peak A are perpendicular to the basal plane of the substrate sheet, while those represented by peak B are parallel to the basal plane. Considering that the orbitals of σ^*_{Si-N} and σ^*_{Si-Cl} are distributed in-plane and out-of-plane, respectively, the observed polarization dependence indicates that the molecular planes are nearly parallel to the surface.

In order to determine more precise tilted angles of the molecular plane with respect to the substrates, the integrated intensities of the σ^*_{Si-Cl} resonance peak were obtained using a curve-fitting technique. Using a nonlinear least-squares routine, the NEXAFS curves were fitted with a linear combination consisting of four symmetrically broadened Gaussian functions for the resonant features and of a Gaussian-broadened step function for the edge jump [28].

For systems with threefold or greater azimuth symmetry, the angle-dependent intensities for the $\sigma^*_{\mathrm{Si-Cl}}$ resonance can be expressed as,

$$I(\theta, \alpha) \propto P(\sin^2\alpha \sin^2\theta + 2\cos^2\alpha\cos^2\theta) + (1 - P)\sin^2\alpha \tag{4}$$

where P is the degree of linear polarization of x-rays and the tilted angle α represents the polar angle of the $\sigma^*_{\mathrm{Si-Cl}}$ orbital, namely the angle between the surface normal ($\vec{n}$) and the $\sigma^*_{\mathrm{Si-Cl}}$ orbital [15].

In the lower sides of figures 4–6, the normalized intensities of the $\sigma^*_{\mathrm{Si-Cl}}$ resonance peak as a function of the incident angle, θ, are shown for the respective samples. Also shown are the results of the curve-fitting analysis using a vector-type equation (4) and three hypothetical α values. Here the error of the tilted angles depends on the absolute value of the angle. For angles near to 0° and 90°, the error is within 1°. However, for angles near to 54.7° (the magic angle), the error becomes larger (about 10°).

The polarization factor (P) of the synchrotron beam under the present experimental conditions is estimated to be about 0.9 [29]. From the plot in figure 4, we obtained that the average tilted angle of the polar angle of the $\sigma^*_{\mathrm{Si-Cl}}$ orbital is 2° on the HOPG substrate. On the other hand, the average tilted angles on gold and ITO are 20° and 26°, respectively. If the molecules are randomly oriented, the average tilted angle should be close to the magic angle, i.e. 54.7°. All of the average tilted angles fairly deviated from the magic angle, which means that the Si–Cl bonds tend to be perpendicular to the surface, while the Si–N bonds tend to lie down on the surface, on average.

It is noted that, although the $SiPcCl_2$ molecules nearly lie down on the three substrates, the precise quantitative analyses showed that the average tilted angles are fairly different between the three substrates. Considering that the three samples were prepared under the same conditions and have the same thicknesses (five layers), we assume that the properties of the surface play an important role in the molecular orientation. Ikame *et al* have reported the orientations of zinc phthalocyanine molecules deposited on gold and magnesium, and found that orientations are different between the two metal substrates [11]. They attributed the observed difference in orientation to the difference in chemical reactivity between gold and magnesium surfaces. In the present case, on the other hand, the observed difference in the molecular orientation is not due to the chemical reactivity, because all of the substrates have chemically inert surfaces and the molecules are attached to the surface through the Van der Waals force. As another factor, we consider that the difference in the tilted angle is due to the differences in the microscopic morphologies of the surfaces.

It is observed that the tilted angle of $SiPcCl_2$ on HOPG is the smallest among the three substrates, and the molecular plane is almost parallel to the surface. This result is deduced from the fact that HOPG has a perfectly flat surface without defects and steps. The lattice constant of the top surface layer of graphite sheet (graphene) is 0.25 nm, which is smaller than the molecular size of $SiPcCl_2$ (1.2 nm). So, even if $SiPcCl_2$ molecules adsorb at specific sites of graphene, a plane structure of this large molecule takes first priority to induce parallel orientation.

Considering that the flatness of the ITO surface is inferior to that of HOPG, it is deduced that the average tilted angle (26°) observed on ITO is due to the roughness of the top surface layer of the ITO. In order to confirm this speculation, the AFM images were observed, which is shown in figure 7. Figure 7(a) shows the differentiated AFM image for the ITO surface. Although the average size of the domains is on the order of 100 nm, smaller domains are also observed between the domains. In figure 7(b), the cross-sectional view of the observed region is displayed. It is seen that the vertical undulation is on the order of 10 nm, which is larger than the molecular size of $SiPcCl_2$. It is deduced that the first layer of $SiPcCl_2$ molecules

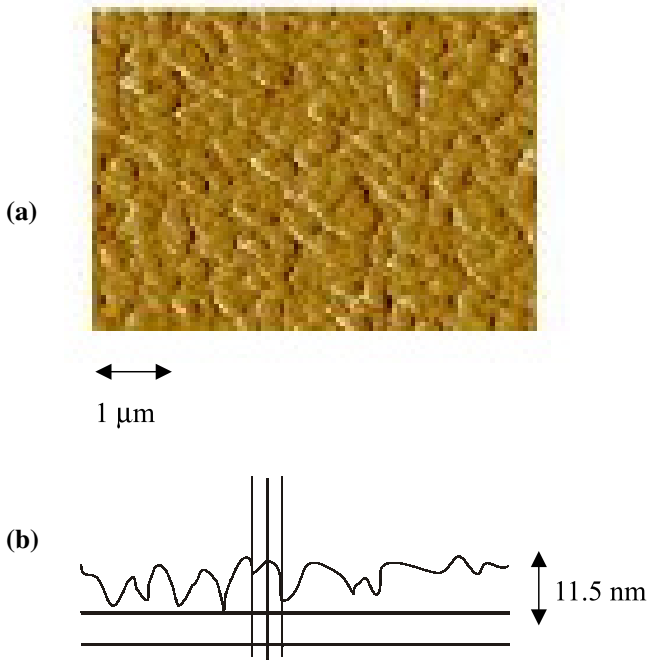

Figure 7. (a) Differentiated AFM images for ITO surface. (b) Cross-sectional view of the image (a).

(This figure is in colour only in the electronic version)

lies down along the morphology of the top surface layer of the substrate. Considering that the thickness of the layer is about five monolayers, the second layer and subsequent layers lie down parallel to the first layer. This means that the orientation of the first layer determines the orientation of the subsequent multilayered films. We conclude that the morphology of the top surface layer of the substrate affects the molecular orientation of multilayered $SiPcCl_2$ films as well as monolayered molecules. This finding is quite important for designing and fabricating multilayered organic thin films. Further analyses based on the AFM observations are now in progress in order to confirm the relation between the surface morphology and the molecular orientations.

4. Summary

We have measured the molecular orientations of $SiPcCl_2$ thin films deposited on three different substrates by NEXAFS spectroscopy using linearly polarized x-rays from a synchrotron light source. The polarization dependences of the Si K-edge NEXAFS spectra showed that the molecular planes of $SiPcCl_2$ deposited on HOPG, Au and ITO substrates tend to be oriented and nearly parallel to the basal plane. A quantitative analysis of the polarization dependence revealed that the molecular orientations in thin films (2.56 nm thick) depend on the substrates. The molecules are almost parallel to the surface (the tilted angle was 2°) on HOPG, while the tilted angle on the ITO surface was 26°. It is concluded that the morphology of the top surface layer of the substrate affects the molecular orientation of multilayered $SiPcCl_2$ films as well as monolayered molecules.

Acknowledgments

The authors would like to express their gratitude to the staff of the KEK-PF for their assistance throughout the experiments. The work was undertaken with the approval of the Photon Factory Program Advisory Committee (proposal no. 2004G340).

References

[1] Friend R H, Gymer R W, Holmes A B, Burroughes J H, Marks R N, Taliani C, Bradley D D C, Dos Santos D A, BréDas J L, LöGdlund M and Salanecket W R 1999 *Nature* **397** 121
[2] Dimitrakopoulos C and Malenfant P R L 2002 *Adv. Mater.* **99** 14
[3] Chizhov I, Scoles G and Kahn A 2000 *Langmuir* **16** 4358
[4] Cox J J, Bayliss S M and Jones T S 1999 *Surf. Sci.* **433** 152
[5] Walzer K and Hietschold M 2001 *Surf. Sci.* **471** 1
[6] Dirk C W, Inable T, Schoch K F Jr and Marks T J 1983 *J. Am. Chem. Soc.* **105** 1539
[7] Michaelis W, Wöhrle D and Schlettwein D 2004 *J. Mater. Res.* **19** 2040
[8] Peisert H, Schwiegerm T, Auerhammerm J M, Knupfer M and Golden M S 2001 *J. Appl. Phys.* **90** 466
[9] Vearey-Roberts A R, Steiner H J, Evans S, Cerrillo I, Mendez J, Cabailh G, Brien S O, Wells J W, McGovern I T and Evans D A 2004 *Appl. Surf. Sci.* **234** 131
[10] Ikame T, Kanai K, Ouchi Y, Ito E, Fujimori A and Seki K 2005 *Chem. Phys. Lett.* **413** 373
[11] Tokito S, Sakata J and Taga Y 1995 *Thin Solid Films* **256** 182
[12] Schlettwein D, Hesse K, Tada H, Mashiko S, Storm U and Binder J 2000 *Chem. Mater.* **12** 989
[13] Naitoh Y, Matsumoto T, Sugiura K, Sakata Y and Kawai T 2001 *Surf. Sci.* **487** L534
[14] Bao Z, Lovinger A J and Brown J 1998 *J. Am. Chem. Soc.* **120** 207
[15] Stöhr J 1992 *NEXAFS Spectroscopy* (Berlin: Springer)
[16] Narioka S, Ishii H, Ouchi Y, Yokoyama T, Ohta T and Seki K 1995 *J. Phys. Chem.* **99** 1332
[17] Okajima T, Narioka S, Tanimura S, Hamano K, Kurata T, Uehara Y, Araki T, Ishii H, Ouchi Y, Seki K, Ogama T and Koezuka H 1996 *J. Electron Spectrosc. Relat. Phenom.* **78** 379
[18] Baba Y, Sekiguchi T and Shimoyama I 2002 *Nucl. Instrum. Methods Phys. Res.* B **194** 41
[19] Criado D, Alayo M I, Fantini M C A and Pereyra I 2006 *J. Non-Cryst. Solids* **352** 1298
[20] Carter W J, Schweitzer G K and Carlson T A 1974 *Electron Spectroscopy* (Amsterdam: Elsevier) p 827
[21] Scofield J H 1973 Theoretical Photoionization Cross Sections from 1 to 1500 keV *UCRL*-51326, Lawrence Livermore Laboratory
[22] Tanuma S, Powell C J and Penn D R 1994 *Surf. Interface Anal.* **21** 165
[23] Miao P, Robinson A W, Palmer R E, Kariuki B M and Harris K D M 2000 *J. Phys. Chem.* B **104** 1285
[24] Boo B H, Liu Z Y and Koyano I 2000 *J. Phys. Chem.* A **104** 1474
[25] Dai B Q and Zhang G L 2002 *Mater. Chem. Phys.* **77** 318
[26] Gomila R M, Quiñonero D, Frontera A, Ballester P and Deyà P M 2000 *J. Mol. Struct.* **531** 38
[27] Sekiguchi T 2006 unpublished results
[28] Outka D A and Stöhr J 1988 *J. Chem. Phys.* **88** 3539
[29] Kitamura H 1993 *Synchrotron Radiation Calculation Program for PC98* version 2.3